applied sciences

MDPI

Article

Development of an Artificial Intelligence-Based System for Predicting Weld Bead Geometry

Ngoc-Hien Tran [1,*], Van-Hung Bui [1] and Van-Thong Hoang [2]

[1] Faculty of Mechanical Engineering, University of Transport and Communications, Hanoi 100000, Vietnam
[2] Faculty of Information Technology, University of Transport and Communications, Hanoi 100000, Vietnam
* Correspondence: tranhien.tkm@utc.edu.vn

Abstract: The prediction of the weld bead geometry parameters is an important aspect of welding processes due to it is related to the strength of the welded joint. This research focuses on using statistical design techniques and a deep learning neural network to predict the weld bead shape parameters of shielded metal arc welding (SMAW), metal inert gas (MIG), and tungsten inert gas (TIG) welding processes. With the statistical design techniques, experiments were carried out to obtain the data for generating the regression models. Establishing mathematical models that shows the relationship between welding process parameters and weld bead size is significant for practical applications. The mathematical model enables the determination of the weld bead size when setting specific welding process parameters. In this research, experimental research results were obtained to build mathematical models showing the relationship between welding process parameters and weld bead geometries for SMAW, MIG, and TIG welding processes. The research results serve as the basis for establishing predictive systems or optimizing welding process parameters. With deep learning neural network techniques, we developed an artificial intelligence-based system for predicting complicated relations between the welding process parameters and the weld bead size. Both a regression model and the deep learning model result in a good correlation between the welding process parameters and the weld bead geometry.

Keywords: predictive system; shielded metal arc welding (SMAW); metal inert gas (MIG); tungsten inert gas (TIG); artificial intelligence; regression model; weld bead geometry

Citation: Tran, N.-H.; Bui, V.-H.; Hoang, V.-T. Development of an Artificial Intelligence-Based System for Predicting Weld Bead Geometry. *Appl. Sci.* **2023**, *13*, 4232. https://doi.org/10.3390/app13074232

Academic Editor: Guijun Bi

Received: 9 March 2023
Revised: 24 March 2023
Accepted: 25 March 2023
Published: 27 March 2023

1. Introduction

The arc-welding processes such as shielded metal arc welding (SMAW), metal inert gas (MIG), and tungsten inert gas (TIG) play an important role in industrial applications [1–3]. The SMAW welding process is a manual arc welding process that uses a consumable electrode coated in flux to lay the weld. The MIG welding process also uses a consumable electrode, while the TIG process uses a non-consumable electrode. Generally, the quality of a weld joint is directly influenced by the welding input parameters. Optimization of process parameters has a great influence on the weld joint quality. To evaluate the weld joint, the weld bead geometry is an important factor. Some methods, including theoretical studies, statistical analysis [4], and artificial intelligence-based prediction systems [5,6], have been used to predict the weld bead shape. Benyounis et al. presented a literature review on the application of design of experiment (factorial design, linear regression, response surface methodology, and Taguchi method), evolutionary algorithms, and computational networks (artificial neural network, simulated annealing, fuzzy clustering technique, and controlled random search) which show the mathematical relationship between the welding process input parameters and the output responses of the weld joint [7].

The generation of a regression model from experiments by applying the regression technique and statistical analysis was proposed and applied in industrial applications. Mohd et al. carried out experiments to develop mathematical models which show the

relationship between the SMAW process parameters (including welding current, arc length, welding speed, welding gap, and electrode diameter) and the weld bead geometry [1]. Mathematical models using the regression technique and statistical analysis were generated to predict the weld bead geometry in the double pulse gas metal arc welding process [8]. Singh et al. considered the effect of the welding current on the weld bead geometry when changing the welding current in experiments [9]. For optimizing the welding parameters in the SMAW process, the factorial design approach was used to establish the relationship between the welding deposition area and the welding voltage, welding current, and welding speed [10]. The MIG welding process with welding speed, voltage, wire feed rate, gas flow rate, nozzle plate distance, and torch angle as the input parameters and weld bead width, weld bead height, and weld bead penetration as the output parameters was analyzed using the regression technique. Both linear and nonlinear regression analyses were employed to establish the input–output relations [2].

Artificial intelligence techniques were applied for predicting the weld bead shape. Ahmed et al. developed a radial basis function neural network (RBF-NN)-based model and a multilayer perceptron neural network (MLP-NN) model for predicting the weld base shape in the SMAW welding process [11]. The results show that the RBF-NN model was able to achieve a high level of accuracy in simulating the weld geometry and very satisfactorily predicted all parameters in comparison with the MLP-NN model. This confirms that the RBF-NN technique is a powerful tool for analysis and modeling [11]. In the SMAW process, research on the effect of the welding process parameters, cryo-treatment, and preheating on the welding characteristics using an artificial neural network (ANN) was carried out [12]. For the SMAW process, Singh et al. used an ANN to predict the weld width in consideration of values of current, voltage, speed of welding, and external magnetic field to produce the best quality of weld with respect to weld width [13].

Integration of regression and artificial intelligence techniques was also proposed for predicting the weld bead in a single welding process. Kuma et al. carried out experiments to generate a linear regression model with welding speed, wire feed rate, % cleaning, gap, and welding current as the input parameters and the weld bead shape as the response in the TIG welding process [6]. A back-propagation neural network also was used for predicting the weld bead shape [6]. Rururaja et al. proposed both a regression model and a machine learning model for predicting the weld bead shape in the gas metal arc welding (GMAW) process with the input parameters including plate thickness, welding current, and welding speed and the weld bead shape as the response [14]. In addition, with the GMAW welding process, Campbell et al. carried out experiments for comparison with the results of the weld bead shape generated by applying ANN. The comparison of experimental and predicted results shows that an ANN-based model can be successfully employed to predict multiple weld geometries [15]. For the TIG welding process, Nagesh et al. developed mathematical models for weld bead shape parameters using the multiple linear regression technique with experimental data. Then, these data also were used to predict the weld bead shape parameters using a back-propagation neural network [16]. Back-propagation with the Levenberg–Marquardt training algorithm was used to train a neural network for predicting the weld bead geometry in laser micro-welding [17]. The The Levenberg–Marquardt training algorithm also was used for predicting weld beads in the SMAW welding process [18]. A neural network and a second-order regression analysis were proposed for predicting bead geometry in robotic gas metal arc welding [19]. In this study, a neural network was adopted to characterize the complex relationship between input variables and the bead geometry. Kim et al. reported research on multiple regression and back-propagation neural network approaches in modeling the top bead height of multi-pass gas metal arc (GMA) welds with the input parameters including pass number, welding current, welding speed, and arc voltage [20]. A deep learning neural network with four-hidden-layer architecture and a sigmoid activation function for estimation of the weld bead parameters in the TIG welding process was proposed by Keshmiri et al. [21].

From the literature review, experiments for generating the mathematical models which show the relationship between the welding process parameters and the weld bead shape were studied. Artificial intelligence techniques for developing models for predicting weld bead shape also were used. However, the integration of a predictive system for predicting the weld bead shape with the SMAW, MIG, and TIG welding processes has not yet been carried out and reported. Currently, we are developing a virtual welding system for training students to have welding skills. The proposed virtual welding system enables learners to practice welding operations. So, they gain welding experience to minimize errors when carrying out real welding. With this purpose, we propose the development of a system that integrates three welding processes, namely the SMAW, MIG, and TIG welding processes. In this paper, we propose the development of a predictive system that enables the prediction of the weld bead information according to the welding process parameters of the SMAW, MIG, and TIG welding processes. This is one part of the whole virtual welding system. In order to consider the effects of the main factors of the welding process, a linear regression technique has been used to develop mathematical models for the weld bead shape parameters of SMAW, MIG, and TIG welding processes.

2. Materials and Methods

2.1. Systematic Procedure for Developing the Predictive System

For developing the predictive system, the systematic procedure is shown in Figure 1. The system enables the prediction of the weld bead shape (including bead width, reinforcement, and penetration) of SMAW, MIG, and TIG welding processes. From analyzing the mechanism of the SMAW, MIG, and TIG welding processes as well as the welding joint types, the input parameters that are the welding process parameters and the allowed values of these parameters were determined. To develop mathematical models showing the relationship between the input parameters and the weld bead shape, experiments were carried out. These experiments are designed by using the factorial design technique. Then, the MiniTab tool was used to establish the relationship between the input parameters and the response. From the established mathematical models, the main factors affecting the weld bead shape were determined. These data were used for training the artificial intelligence (AI)-based models. For developing the AI-based model, the network architecture for SMAW, MIG, and TIG welding process with the input layer including the welding process parameters and the output layer that is the weld bead shape was used. The deep learning technique and Python platform were used for programming modules for the predictive system. These modules include interface, SMAW, MIG, and TIG modules.

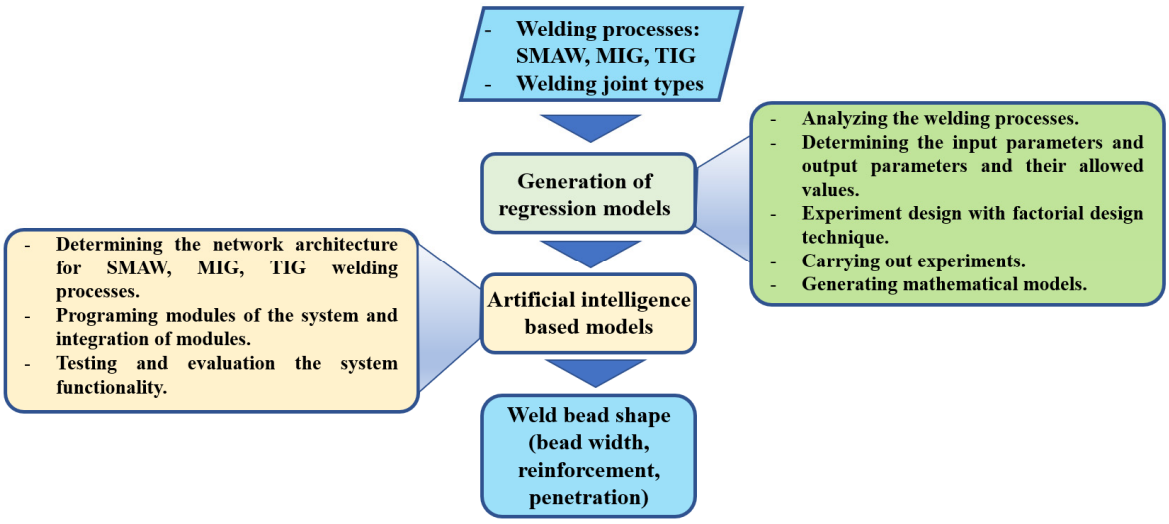

Figure 1. Systematic procedure for developing the predictive system.

2.2. SMAW, MIG, and TIG Welding Processes

The mechanism of the shielded metal arc welding (SMAW) process is shown in Figure 2. The SMAW process uses a flux-coated consumable electrode with a metal rod at the core. The arc between the electrode and the base metal plate creates the required heat for generating the weld bead [22].

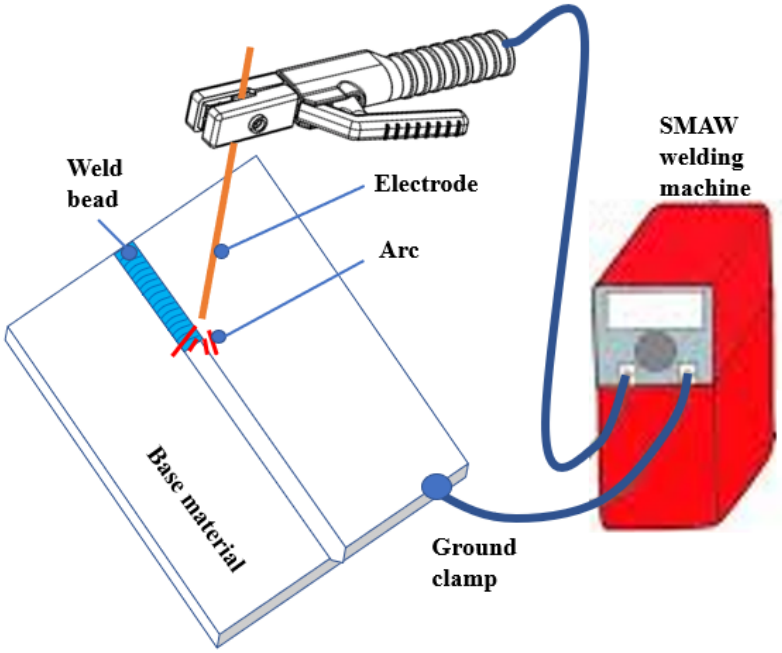

Figure 2. Mechanism of SMAW welding process.

Figure 3 shows the mechanism of the tungsten inert gas (TIG) welding process. The TIG process uses a power source, a shielding gas, and a tungsten inert gas torch. The TIG welding process is used to produce weld joints with a non-consumable tungsten electrode. In some cases, the filler rod is used to have the added material to fill up the gap between two joints. In the TIG welding process, the arc is formed between a pointed tungsten electrode and the base material plate in an inert gas such as argon (Ar), helium (He), or an Ar–He mixture [23].

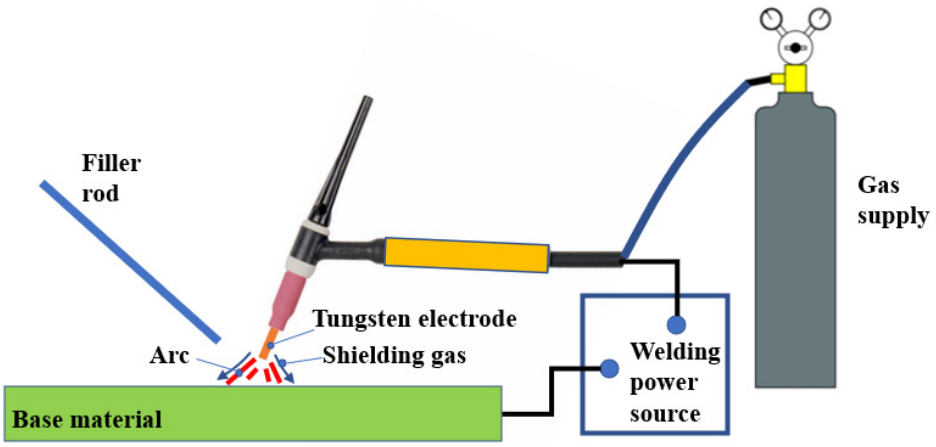

Figure 3. Mechanism of TIG welding process.

Figure 4 shows the mechanism of the MIG welding process. The MIG process uses a power source, a shielding gas, and a consumable wire electrode. In the MIG welding process, the arc melts the electrode wire to add the material to the base metal plates. The shielding gas keeps the weld pool free from atmospheric contamination.

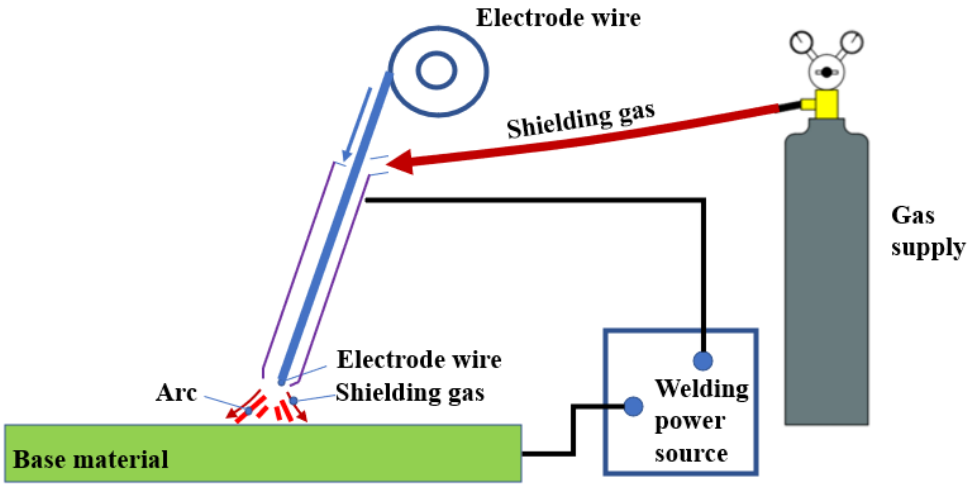

Figure 4. Mechanism of MIG welding process.

2.3. Experiments for Generating Data and Development of Regression Models

Experiments were conducted on the SMAW, MIG, and TIG welding machines. For carrying out SMAW, MIG, and TIG welding processes, we used ARC 200, MIG 200, and TIG 200 welding machines, respectively. For carrying out the experiments, the welding process parameters that highly influence the quality of weld joints were selected. The ranges of welding process parameters and experimental results are shown in Tables 1–6 for the SMAW, MIG, and TIG welding process, respectively. These ranges were selected according to the specification of machines, base material, and electrode material and consideration of the welding experiments as well as the reported research on the SMAW, MIG, and TIG welding processes [1–3]. The two-level full factorial design method was used for designing experiments and generating mathematical models [24,25]. With the SMAW welding process, the input process parameters that highly influence the quality of weld joints include welding current, welding speed, arc length, electrode diameter, and welding gap. The values for the SMAW welding process are shown in Table 1. Base metal plates in a square butt weld joint with a flat position are structural mild steel plates; the thickness of each plate is 6 mm.

Table 1. Input parameters for SMAW process [1].

Parameter	Unit	Notation	Minimum Value (−)	Maximum Value (+)
Welding current	A	*A*	60	90
Arc length	mm	*B*	1.2	3.0
Welding speed	mm/min	*C*	70	120
Electrode diameter	mm	*D*	2.6	4.0
Joint gap	mm	*E*	1.0	3.0

To obtain regression models which show the relationship between the input parameters and the weld bead size as shown in Figure 5, the two-level full factorial design method was used to create a design matrix for this experiment. With 2 levels and 5 parameters, a total of 32 experiments were conducted as shown in Table 2.

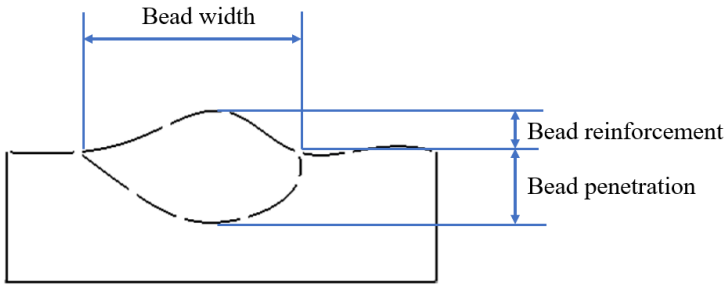

Figure 5. Geometry of weld bead.

Table 2. Experimental design and weld bead size for SMAW welding.

Number	*A*	*B*	*C*	*D*	*E*	K_S (mm)	R_S (mm)	P_S (mm)
1	60	3.0	70	4.0	3.0	9.6	1.0	1.4
2	90	1.2	70	2.6	3.0	10.9	1.5	1.3
3	60	1.2	120	2.6	3.0	9.3	2.0	1.3
4	60	3.0	120	4.0	1.0	9.0	0.8	1.5
5	90	3.0	120	4.0	3.0	8.1	1.1	1.6
6	90	1.2	70	4.0	1.0	8.0	1.8	1.5
7	90	3.0	70	2.6	3.0	9.3	1.0	1.4
8	60	1.2	120	2.6	1.0	11.3	1.5	1.3
9	60	3.0	70	4.0	1.0	9.0	2.0	1.4
10	90	1.2	120	2.6	3.0	7.8	1.0	1.7
11	60	1.2	120	4.0	3.0	10.2	1.3	2.5
12	90	3.0	120	4.0	1.0	7.7	1.4	1.9
13	60	3.0	120	2.6	1.0	7.4	1.2	2.2
14	90	3.0	120	2.6	1.0	8.9	1.7	2.2
15	60	3.0	70	2.6	3.0	11.3	1.6	1.7
16	90	1.2	120	4.0	3.0	8.5	1.0	2.2
17	60	3.0	70	2.6	1.0	8.5	1.3	2.3
18	90	3.0	70	2.6	1.0	9.7	1.6	1.8
19	60	1.2	70	4.0	3.0	9.4	1.4	2.2
20	90	1.2	70	4.0	3.0	10.9	1.3	1.6
21	60	1.2	70	2.6	3.0	7.4	1.8	2.0
22	90	1.2	120	4.0	1.0	9.4	1.2	2.6
23	60	1.2	70	2.6	1.0	8.5	0.9	2.2
24	60	3.0	120	4.0	3.0	10.1	1.6	2.1
25	60	1.2	70	4.0	1.0	10.0	1.4	2.4
26	90	3.0	70	4.0	3.0	11.0	1.5	2.3
27	60	3.0	120	2.6	3.0	10.6	2.0	2.3
28	90	3.0	70	4.0	1.0	10.2	0.8	2.4
29	90	1.2	70	2.6	1.0	8.5	1.1	2.6
30	60	1.2	120	4.0	1.0	9.7	1.8	2.4
31	90	3.0	120	2.6	3.0	9.9	1.0	2.9
32	90	1.2	120	2.6	1.0	8.9	0.6	2.6

In consideration of the independent effects of welding process parameters and the linear regression model, the weld bead dimensions in the SMAW welding process including bead width (K_S), reinforcement (R_S), and penetration (P_S) are calculated as follows:

$$K_S = 9.41 - 0.0072\,A + 0.064\,B - 0.00697\,C + 0.123\,D + 0.293\,E \quad (1)$$

$$R_S = 2.094 - 0.00826\,A - 0.0044\,B - 0.00102\,C - 0.022\,D + 0.0285\,E \quad (2)$$

$$P_S = 1.707 + 0.00272\,A - 0.0406\,B + 0.00351\,C + 0.007\,D - 0.0942\,E \quad (3)$$

For the MIG welding process, the input process parameters include welding speed, arc voltage, wire feed rate, gas flow rate, nozzle-to-plate distance, and torch angle. The values for the MIG welding process are shown in Table 3. Base metal plates are structural mild steel plates; the thickness of each plate is 8 mm.

Table 3. Input parameters for MIG process [2].

Parameter	Unit	Notation	Minimum Value (−)	Maximum Value (+)
Welding speed	cm/min	*a*	25	45
Arc voltage	V	*b*	26	30
Wire feed rate	m/min	*c*	6	7
Gas flow rate	L/min	*d*	14	18
Nozzle-to-plate distance	mm	*e*	15	20
Torch angle	degree	*f*	70	100

With 2 levels and 6 parameters, a total of 64 experiments were conducted as shown in Table 4.

Table 4. Experimental design and weld bead size for MIG welding.

Number	*a*	*b*	*c*	*d*	*e*	*f*	K_M (mm)	R_M (mm)	P_M (mm)
1	45	30	6	18	20	100	9.2	2.4	1.8
2	25	30	6	18	15	70	11.6	3.4	2.5
3	45	26	7	18	20	70	7.6	3.4	2.0
4	25	26	7	14	20	100	9.4	3.9	1.9
5	45	30	6	14	20	100	9.2	2.4	1.7
6	45	30	7	18	20	100	9.8	2.6	2.0
7	25	26	7	18	15	100	9.8	3.8	2.0
8	45	30	7	18	15	100	10.1	2.5	2.1
9	25	26	6	14	20	70	8.8	4.0	2.0
10	45	30	6	14	15	70	9.4	2.6	2.1
11	25	30	6	14	20	70	11.2	3.5	2.4
12	45	30	7	18	20	70	9.7	2.9	2.4
13	45	30	6	14	20	70	9.1	2.7	2.1
14	25	26	7	18	15	70	9.7	4.1	2.4
15	25	26	6	18	20	70	8.9	4.0	2.1
16	45	26	7	14	20	100	7.6	3.2	1.6
17	25	30	7	14	20	70	11.9	3.6	2.7

Table 4. *Cont.*

Number	*a*	*b*	*c*	*d*	*e*	*f*	K_M (mm)	R_M (mm)	P_M (mm)
18	25	26	6	14	15	100	9.1	3.7	1.7
19	25	30	7	14	15	100	12.4	3.2	2.3
20	45	30	7	18	15	70	10.0	2.8	2.5
21	45	26	6	18	20	70	7.2	3.3	1.8
22	45	26	7	14	15	100	7.9	3.1	1.6
23	25	26	7	14	20	70	9.3	4.2	2.3
24	45	26	7	18	15	100	7.9	3.0	1.7
25	25	30	7	14	15	70	12.3	3.5	2.7
26	25	30	7	18	20	100	12.1	3.3	2.3
27	25	30	7	18	20	70	12.0	3.6	2.7
28	45	26	7	18	20	100	7.7	3.1	1.7
29	45	26	6	14	15	100	7.4	2.9	1.4
30	25	26	7	14	15	70	9.6	4.1	2.3
31	45	26	6	14	15	70	7.3	3.2	1.7
32	45	30	7	14	15	100	10.0	2.5	2.0
33	25	30	7	18	15	70	12.3	3.5	2.8
34	45	26	7	18	15	70	7.8	3.3	2.1
35	25	26	7	14	15	100	9.7	3.8	1.9
36	45	30	7	14	15	70	9.9	2.8	2.4
37	45	26	6	18	15	100	7.4	2.9	1.4
38	45	30	6	18	15	100	9.5	2.3	1.8
39	25	30	7	14	20	100	12.0	3.3	2.3
40	45	26	6	18	20	100	7.2	3.0	1.4
41	25	26	7	18	20	70	9.4	4.2	2.4
42	45	26	7	14	20	70	7.6	3.5	2.0
43	25	26	6	14	15	70	9.0	4.0	2.1
44	25	30	6	18	15	100	11.7	3.1	2.1
45	45	30	6	18	20	70	9.2	2.7	2.2
46	25	30	6	18	20	100	11.4	3.2	2.1
47	25	26	7	18	20	100	9.5	3.9	2.0
48	45	26	6	14	20	100	7.2	3.0	1.3
49	25	26	6	18	15	100	9.2	3.6	1.7
50	45	26	6	14	20	70	7.1	3.3	1.7
51	25	26	6	18	20	100	8.9	3.7	1.7
52	25	30	6	18	20	70	11.3	3.5	2.5
53	25	26	6	18	15	70	9.1	3.9	2.1
54	45	26	7	14	15	70	7.8	3.4	2.0
55	25	30	6	14	15	100	11.6	3.1	2.0
56	45	30	6	14	15	100	9.4	2.3	1.7

Table 4. *Cont.*

Number	*a*	*b*	*c*	*d*	*e*	*f*	K_M (mm)	R_M (mm)	P_M (mm)
57	25	30	7	18	15	100	12.5	3.2	2.4
58	45	30	7	14	20	100	9.8	2.6	2.0
59	45	30	6	18	15	70	9.4	2.6	2.2
60	45	26	6	18	15	70	7.4	3.2	1.8
61	25	30	6	14	15	70	11.6	3.4	2.4
62	45	30	7	14	20	70	9.7	2.9	2.4
63	25	26	6	14	20	100	8.9	3.7	1.6
64	25	30	6	14	20	100	11.3	3.2	2.0

The linear regression model for calculating the weld bead dimensions in the MIG welding process including bead width (K_M), reinforcement (R_M), and penetration (P_M) are as follows:

$$K_M = -6.502 - 0.1\,a + 0.57969\,b + 0.5813\,c + 0.01562\,d - 0.05375\,e + 0.00271\,f \quad (4)$$

$$R_M = 8.1234 - 0.037187\,a - 0.14219\,b + 0.15625\,c - 0.00469\,d + 0.01875\,e - 0.01\,f \quad (5)$$

$$P_M = -0.9703 - 0.015312\,a + 0.09531\,b + 0.275\,c + 0.01875\,d - 0.005\,e - 0.013125\,f \quad (6)$$

For the TIG welding process, the input process parameters include welding speed, arc voltage, wire feed rate, % cleaning, joint gap, and welding current. The values for TIG welding process are shown in Table 5.

Table 5. Input parameters for TIG process [3].

Parameter	Unit	Notation	Minimum Value (−)	Maximum Value (+)
Welding speed	cm/min	*M*	24	46
Wire feed rate	cm/min	*N*	1.5	2.5
% cleaning		*O*	30	70
Joint gap	mm	*P*	2.4	3.2
Welding current	A	*Q*	80	110

Two structural mild steel plates with 6 mm thickness were used for experiments. With 2 levels and 5 parameters, a total of 32 experiments were conducted as shown in Table 6.

Table 6. Experimental design and weld bead size for TIG welding.

Number	M	N	O	P	Q	K_T (mm)	R_T (mm)	P_T (mm)
1	46	1.5	30	2.4	110	6.1	0.8	2.6
2	46	2.5	70	3.2	80	5.3	1.4	1.4
3	24	2.5	30	3.2	110	12.3	0.4	2.1
4	46	1.5	30	3.2	110	7.3	0.7	1.6
5	24	1.5	70	3.2	110	12.9	0.3	1.9
6	24	2.5	30	2.4	80	6.7	1.2	1.7

Table 6. *Cont.*

Number	M	N	O	P	Q	K_T (mm)	R_T (mm)	P_T (mm)
7	46	2.5	70	2.4	110	7.0	0.8	1.7
8	46	1.5	70	2.4	110	7.7	0.8	1.5
9	46	2.5	70	3.2	110	7.8	0.6	1.8
10	24	1.5	30	2.4	110	11.3	0.4	1.8
11	46	1.5	30	2.4	80	5.0	1.4	1.0
12	46	1.5	70	3.2	110	7.6	0.6	1.5
13	24	1.5	70	2.4	80	7.4	0.8	1.6
14	46	2.5	30	2.4	110	6.4	1.0	1.5
15	24	1.5	30	2.4	80	6.1	0.9	1.7
16	24	2.5	70	2.4	110	11.8	0.4	2.1
17	24	1.5	70	3.2	80	7.3	0.7	1.6
18	46	2.5	30	3.2	80	5.0	1.5	1.1
19	24	2.5	30	3.2	80	6.8	1.1	1.8
20	46	1.5	70	2.4	80	5.0	1.1	1.3
21	24	2.5	70	2.4	80	7.0	0.9	1.9
22	24	1.5	30	3.2	110	11.5	0.3	2.1
23	24	2.5	70	3.2	80	7.5	0.9	1.8
24	46	2.5	70	2.4	80	5.2	1.4	1.4
25	46	1.5	70	3.2	80	4.4	1.1	1.4
26	24	2.5	30	2.4	110	9.3	0.8	1.9
27	46	1.5	30	3.2	80	4.9	1.2	1.3
28	24	2.5	70	3.2	110	12.5	0.4	2.1
29	24	1.5	30	3.2	80	6.4	1.0	1.4
30	46	2.5	30	3.2	110	6.9	1.1	1.5
31	24	1.5	70	2.4	110	11.2	0.7	1.5
32	46	2.5	30	2.4	80	4.8	1.4	1.1

The linear regression models for calculating the weld bead dimensions in TIG welding process including bead width (K_T), reinforcement (R_T), and penetration (P_T) are as follows:

$$K_T = -0.79 - 0.1468\,M + 0.01713\,O + 0.654\,P + 0.1146\,Q \quad (7)$$

$$R_T = 1.978 + 0.0157\,M + 0.1601\,N - 0.00317\,O - 0.099\,P - 0.01625\,Q \quad (8)$$

$$P_T = 0.835 - 0.0157\,M + 0.0738\,N + 0.00034\,O + 0.029\,P + 0.01174\,Q \quad (9)$$

2.4. Modeling of Artificial Intelligence-Based Predictive System

From the regression models, the main welding process parameters of SMAW, MIG, and TIG welding processes were determined. For developing the predictive system, the deep learning neural network (DLNN) was applied. There are many types of layers for the deep learning model depending on the application. In this research, we used the dense layer which is deeply connected with its preceding layer [26]. The network architectures of the TIG and SMAW welding processes are listed in Table 7 and shown in Figures 6 and 7, respectively.

In this DLNN, the rectified linear unit (ReLU) activation function is used. The ReLU is a nonlinear function or piecewise linear function that will output the input directly if it is positive; otherwise, it will output zero. This ReLU activation function is easier to train and often achieves better performance than sigmoid and tanh [27,28].

Mathematically, with x variable and function f, the ReLU function is expressed as follows:

$$f(x) = max\ (0, x) \tag{10}$$

It has become the default activation function for many types of neural networks because a model that uses it is easier to train and often achieves better performance.

Table 7. Network architecture of TIG and SMAW welding processes.

Layer	Layer (Type)	Output Shape	Activation	Param #
Input	Dense	5		
Hidden	dense (Dense)	(None, 64)	ReLU	448
	dense_1 (Dense)	(None, 32)	ReLU	2080
	dense_2 (Dense)	(None, 16)	ReLU	528
	dense_3 (Dense)	(None, 8)	ReLU	136
Output	dense_4 (Dense)	(None, 3)	Linear	27

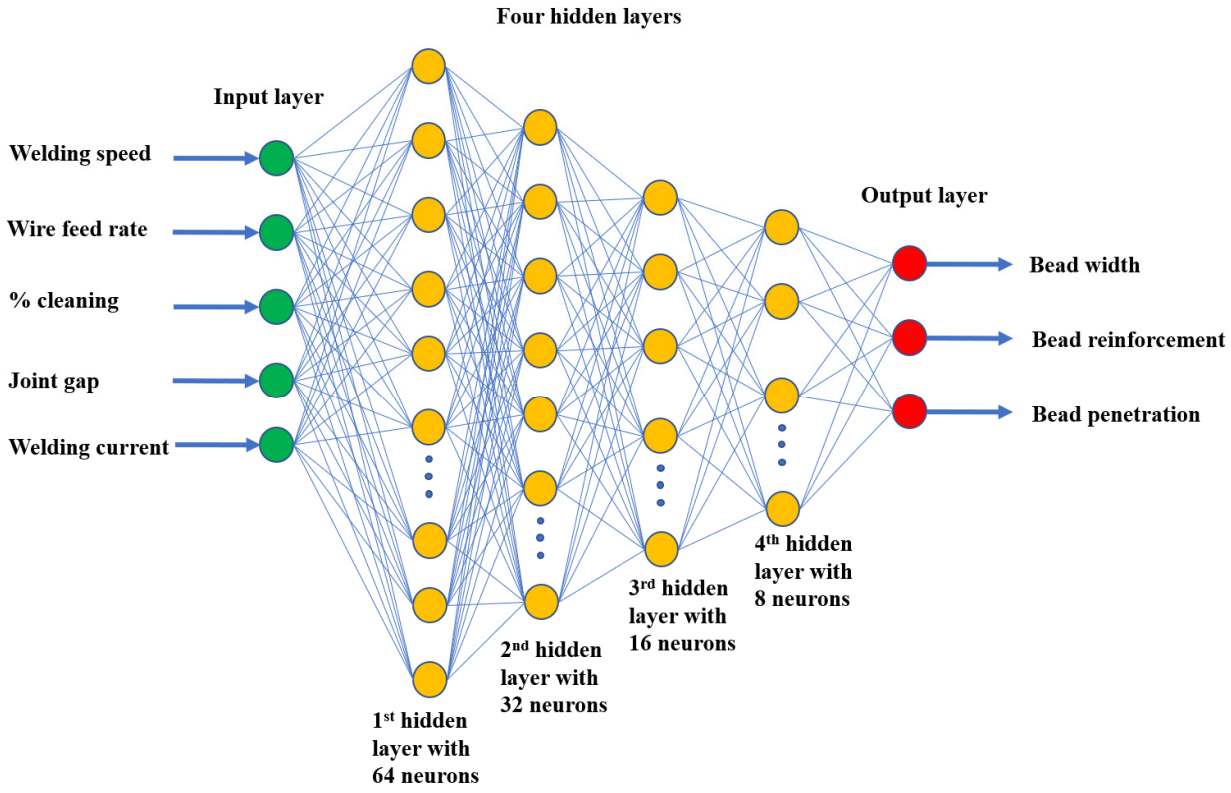

Figure 6. Deep learning neural network architecture for the TIG welding process.

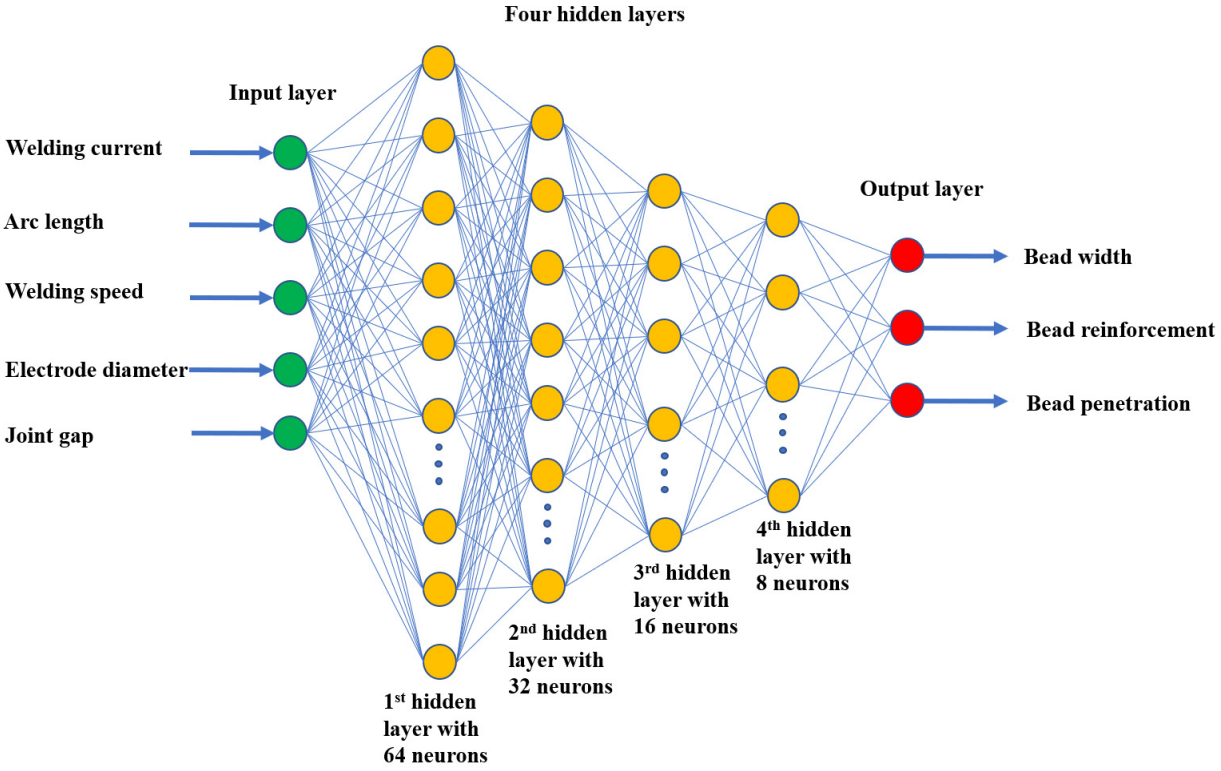

Figure 7. Deep learning neural network architecture for the SMAW welding process.

The network architecture of the MIG welding process is listed in Table 8 and shown in Figure 8. The loss function used in the network is mean squared error (MSE). MSE is calculated as the average of the squared differences between the predicted and actual values [29]; the optimization method is Adam, which is a method for first-order gradient-based optimization of stochastic objective functions [30]. The number of epochs is 10,000 and the batch size is 2. Table 9 shows the parameters for the training network and the root mean squared error (RMSE) of the training set and test set for the TIG, MIG, and SMAW welding processes.

Table 8. Network architecture of MIG welding process.

Layer	Layer (Type)	Output Shape	Activation	Param #
Input	Dense	6		
Hidden	dense (Dense)	(None, 64)	ReLU	448
	dense_1 (Dense)	(None, 32)	ReLU	2080
	dense_2 (Dense)	(None, 16)	ReLU	528
	dense_3 (Dense)	(None, 8)	ReLU	136
Output	dense_4 (Dense)	(None, 3)	Linear	27

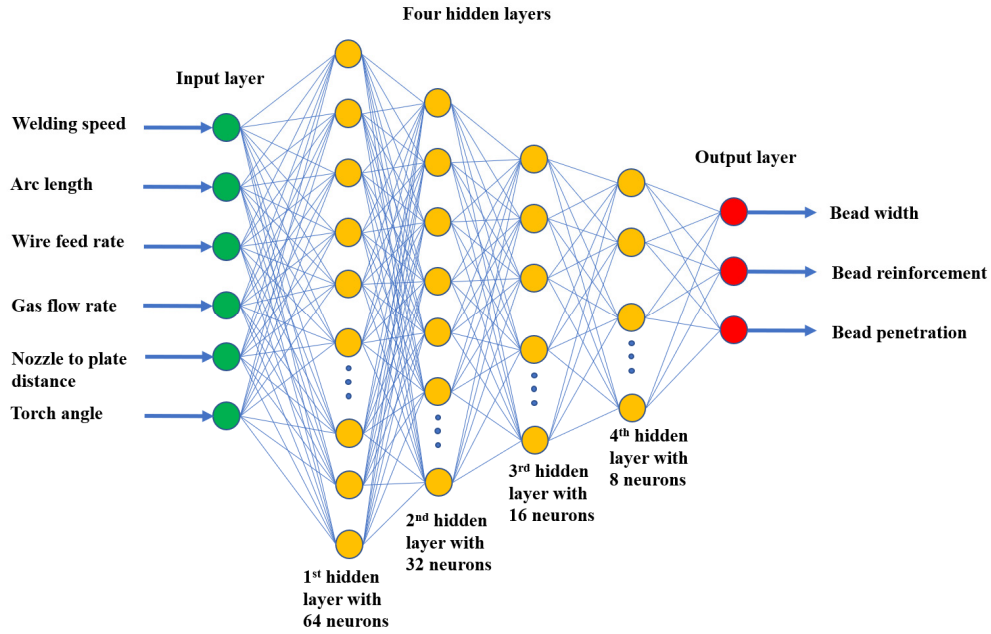

Figure 8. Deep learning neural network architecture for the MIG welding process.

Table 9. Parameters for training network and root mean squared error (RMSE).

Dataset	Number Patterns	Number Patterns of Test Set	Number Patterns of Training Set	RMSE Training Set			RMSE Test Set		
				K	R	P	K	R	P
TIG	128	115	13	0.02625	0.00073	0.00999	0.04818	0.00067	0.00115
MIG	19	98	11	0.00046	0.00009	0.00006	0.00013	0.00020	0.00005
SMAW	62	55	7	0.01049	0.00091	0.00161	0.00220	0.00026	0.00050

3. Results and Discussions

3.1. Implementation of the Artificial Intelligence-Based System

The predictive system with four modules was developed using the Python platform. The interface of the system is shown in Figure 9 with the functions of predicting the weld bead of the TIG, SMAW, and MIG welding process.

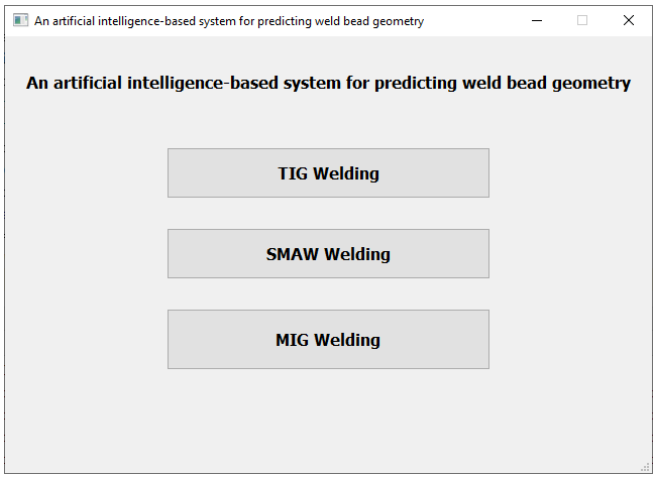

Figure 9. Screenshot of the interface module of the developed predictive system.

The function of predicting the weld bead shape in the TIG welding process was developed, as shown in Figure 10, in which the input process parameters include welding speed, wire feed rate, % cleaning, gap, and current. The response is the weld bead shape.

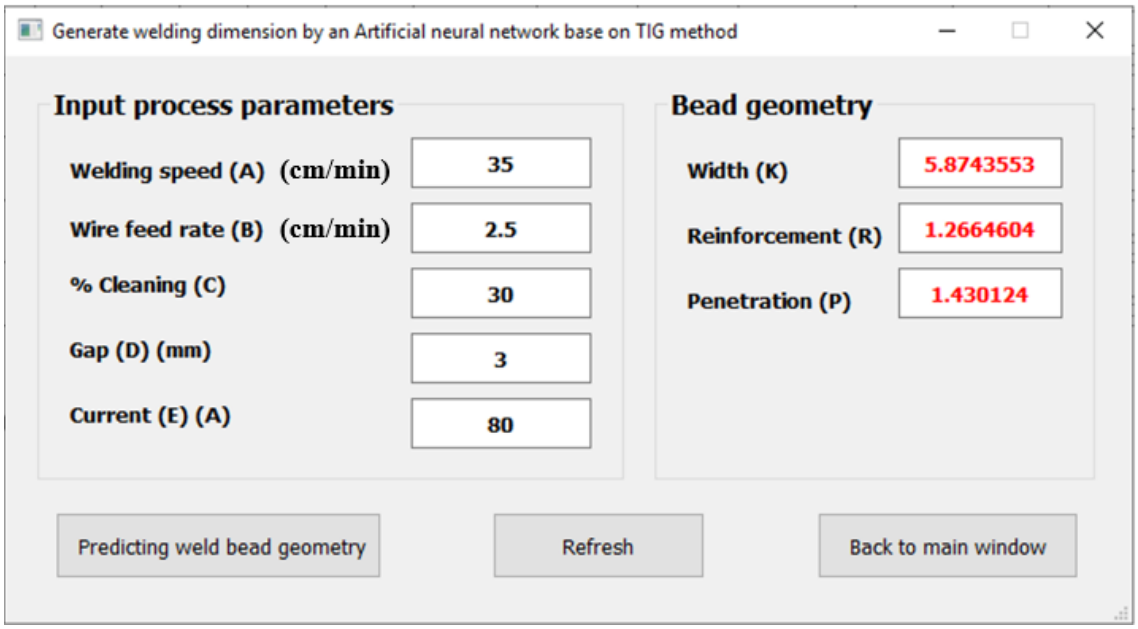

Figure 10. Screenshot of the TIG welding module of the developed predictive system.

Figure 11 shows the module for predicting the weld bead shape in the MIG welding process with the input including welding speed, arc voltage, wire feed rate, gas flow rate, nozzle-to-plate distance, and torch angle. The SMAW module is shown in Figure 12 with welding current, arc length, welding speed, electrode diameter, and joint gap as the input. These figures also show the input parameter values and the output.

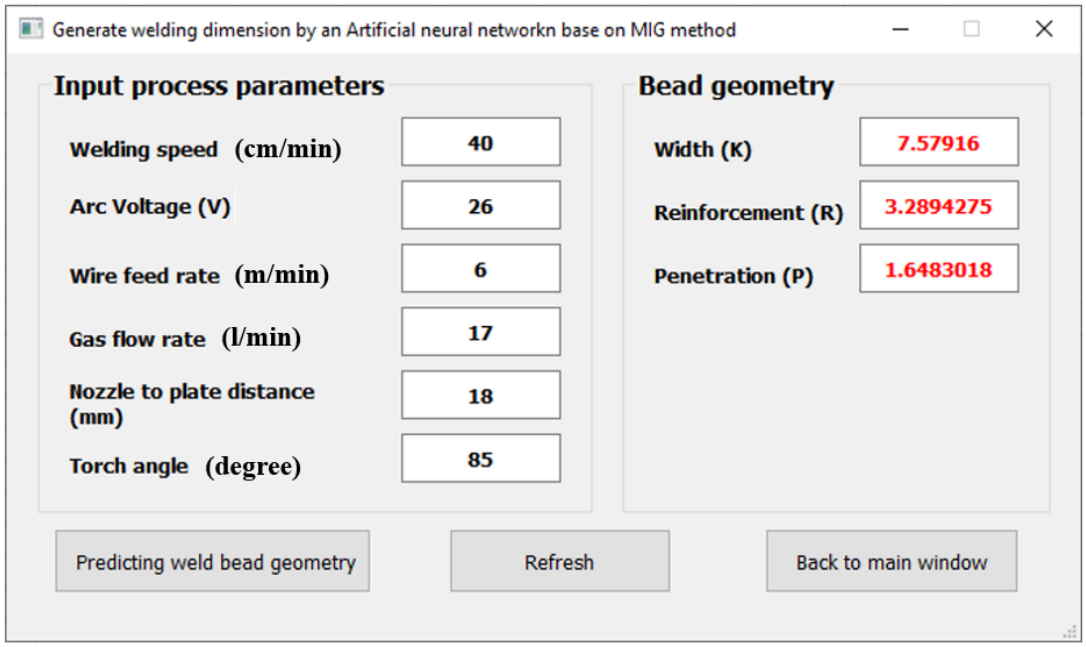

Figure 11. Screenshot of the MIG welding module of the developed predictive system.

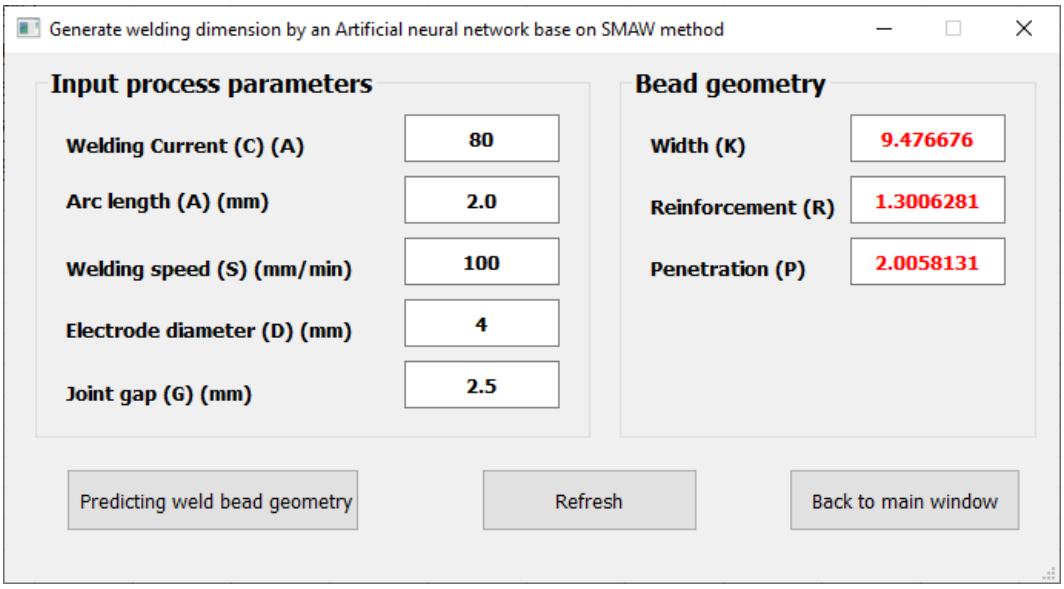

Figure 12. Screenshot of the SMAW welding module of the developed predictive system.

3.2. Testing and Evaluating the Functionality of the Developed Predictive System

The functionality of the developed system was tested successfully. The predicted results are reliable in comparison with the experimental results and the calculated results. Table 10 shows the prediction results of the developed system for the TIG welding process, in which P-K_T, P-R_T, and P-P_T are the predicted weld bead width, reinforcement, and penetration, respectively. C-K_T, C-R_T, and C-P_T are the weld bead width, reinforcement, and penetration calculated by using Equations (7), (8), and (9), respectively. Dev. of K_T, Dev. of R_T, and Dev. of P_T are the deviations between the prediction and calculation results of the weld bead width, reinforcement, and penetration, respectively. The % of K_T, % of R_T, and % of P_T are the deviations between the prediction and calculation results of the weld bead width, reinforcement, and penetration in % for the TIG welding process, respectively.

Table 10. Testing and comparing the prediction and calculation results for the TIG welding process.

M	N	O	P	Q	C-K_T	C-R_T	C-P_T	P-K_T	P-R_T	P-P_T	Dev. of K_T	% of K_T	Dev. of R_T	% of R_T	Dev. of P_T	% of P_T
24	2.5	30	3.2	80	7.46	1.04	1.68	7.80	1.09	1.69	0.33	4.49	0.05	4.58	0.01	0.44
24	2.5	30	2.4	110	10.38	0.63	2.01	10.60	0.62	1.90	0.23	2.19	−0.01	2.22	−0.11	5.55
24	2.5	70	3.2	95	9.87	0.67	1.87	9.94	0.65	1.93	0.08	0.79	−0.03	3.73	0.06	3.08
46	2.5	30	3.2	95	5.95	1.14	1.52	5.91	1.17	1.45	−0.04	0.61	0.03	2.42	−0.06	4.09
24	2	40	2.6	90	8.39	0.83	1.75	8.35	0.83	1.74	−0.04	0.42	0.00	0.04	−0.01	0.79
35	2.5	70	2.4	95	7.73	0.92	1.68	7.73	0.95	1.72	0.01	0.09	0.03	3.24	0.05	2.71
35	2	60	3	105	9.09	0.65	1.77	9.04	0.64	1.76	−0.05	0.56	−0.01	1.76	−0.02	1.01
35	2	50	2.8	85	6.50	1.03	1.53	6.52	1.03	1.50	0.02	0.27	−0.01	0.50	−0.03	2.13
35	1.5	70	2.4	110	9.45	0.52	1.78	9.44	0.50	1.82	−0.01	0.07	−0.02	3.97	0.04	2.45
46	1.5	70	2.4	110	7.83	0.69	1.61	7.70	0.69	1.58	−0.13	1.62	0.00	0.41	−0.02	1.51
30	2.5	50	2.8	95	8.38	0.87	1.76	8.32	0.87	1.74	−0.06	0.73	0.00	0.50	−0.03	1.48
46	1.5	30	2.4	95	5.43	1.06	1.42	5.53	1.08	1.38	0.10	1.90	0.01	1.08	−0.04	2.90
24	1.5	70	3.2	95	9.87	0.51	1.80	9.97	0.51	1.77	0.10	1.06	0.00	0.73	−0.03	1.51

Table 11 shows the prediction and calculation results for the MIG welding process, in which P-K_M, P-R_M, and P-P_M are the predicted weld bead width, reinforcement, and penetration, respectively. C-K_M, C-R_M, and C-P_M are the weld bead width, reinforcement, and penetration calculated by using Equations (4), (5), and (6), respectively. Dev. of K_M, Dev. of R_M, and Dev. of P_M are the deviations between the prediction and calculation results of the weld bead width, reinforcement, and penetration, respectively. The % of K_M, % of R_M, and % of P_M are the deviations between the prediction and calculation results of the weld bead width, reinforcement, and penetration in % for the MIG welding process, respectively.

Table 11. Testing and comparing the prediction and calculation results for MIG welding process.

a	*b*	*c*	*d*	*e*	*f*	C-K_M	C-R_M	C-P_M	P-K_M	P-R_M	P-P_M	Dev. of K_M	% of K_M	Dev. of R_M	% of R_M	Dev. of P_M	% of P_M
25	30	7	18	17	70	12.01	3.56	2.76	9.91	2.82	2.43	−0.10	0.84	−0.14	3.85	−0.13	4.75
40	28	7	17	16	75	9.12	3.14	2.13	8.97	3.14	2.11	−0.15	1.59	0.00	0.11	−0.01	0.62
35	26	6	16	15	70	8.19	3.57	1.93	8.06	3.56	1.93	−0.13	1.58	−0.01	0.20	0.00	0.03
30	27	7	15	16	90	9.84	3.59	2.09	9.85	3.58	2.08	0.02	0.16	−0.01	0.20	−0.01	0.33
30	30	7	15	17	95	11.54	3.13	2.30	11.46	3.12	2.29	−0.07	0.61	−0.01	0.46	−0.01	0.59
25	30	7	14	20	95	11.86	3.38	2.35	12.03	3.36	2.33	0.17	1.42	−0.02	0.64	−0.01	0.63
45	30	7	18	17	80	10.04	2.71	2.33	9.94	2.72	2.30	−0.11	1.06	0.01	0.29	−0.03	1.10
25	26	6	14	15	100	9.24	3.65	1.65	9.22	3.62	1.64	−0.02	0.18	−0.03	0.72	−0.01	0.48
45	26	6	18	18	90	7.12	3.04	1.53	7.31	3.04	1.53	0.20	2.74	−0.01	0.19	−0.01	0.58
30	26	6	15	15	75	8.69	3.71	1.92	8.51	3.70	1.92	−0.18	2.06	−0.01	0.35	0.00	0.02
25	26	7	14	15	100	9.82	3.81	1.92	9.83	3.79	1.92	0.01	0.06	−0.01	0.37	0.00	0.13

Table 12 shows the prediction and calculation results for the SMAW welding process, in which P-K_S, P-R_S, and P-P_S are the predicted weld bead width, reinforcement, and penetration, respectively. C-K_S, C-R_S, and C-P_S are the weld bead width, reinforcement, and penetration calculated by using Equations (1), (2), and (3), respectively. Dev. of K_S, Dev. of R_S, and Dev. of P_S are the deviations between the prediction and calculation results of the weld bead width, reinforcement, and penetration, respectively. The % of K_S, % of R_S, and% of P_S are the deviations between the prediction and calculation results of the weld bead width, reinforcement, and penetration in % for the SMAW welding process, respectively.

Table 12. Testing and comparing the prediction and calculation results for SMAW welding process.

A	*B*	*C*	*D*	*E*	C-K_S	C-R_S	C-P_S	P-K_S	P-R_S	P-P_S	Dev. of K_S	% of K_S	Dev. of R_S	% of R_S	Dev. of P_S	% of P_S
65	2	80	3.5	1	9.24	1.42	2.01	9.26	1.41	2.04	0.02	0.23	−0.01	0.41	0.03	1.31
90	1.5	95	4	2	9.27	1.22	2.06	9.63	1.20	1.98	0.36	3.87	−0.02	1.39	−0.08	3.98
75	1.5	115	4	2	9.24	1.32	2.09	9.21	1.30	2.10	−0.03	0.35	−0.02	1.70	0.01	0.53
80	2.5	90	3	2.5	9.47	1.34	1.92	9.44	1.33	1.91	−0.02	0.26	−0.01	0.57	−0.01	0.54
60	1.2	95	2.6	1	9.01	1.47	2.08	8.81	1.44	1.99	−0.19	2.15	−0.02	1.69	−0.09	4.16
80	1.2	120	4	2	9.15	1.27	2.14	9.21	1.32	2.10	0.06	0.63	0.05	3.60	−0.03	1.57
70	1.5	115	4	1.5	9.13	1.35	2.13	9.02	1.37	2.12	−0.11	1.23	0.03	1.87	0.00	0.13

3.3. Discussion of the Predicted and Calculated Results

Depending on the welding process parameters for SMAW, MIG, and TIG, the weld bead geometries are different for these welding processes. With the range of the proposed welding process parameters, the weld bead geometries predicted by the developed system are suitable in comparison between SMAW, MIG, and TIG welding processes. With the TIG

welding process, maximum of the deviation between the predicted and calculated results is 0.33 mm (or 4.49%) for the weld bead width, 0.05 mm (or 4.58%) for the reinforcement, and 0.11 mm (or 5.55%) for the penetration. The maximum is 0.2 mm (or 2.74%), 0.14 mm (or 3.85%), and 0.13 mm (or 4.75%) for the deviation between the predicted and calculated results of the weld bead width, the reinforcement, and the penetration in the MIG welding process, respectively. With the SMAW welding process, it is 0.36 mm (or 3.87%), 0.05 mm (or 3.6%), and 0.09 mm (or 4.16%) for the deviation between the predicted and calculated results of the weld bead width, the reinforcement, and the penetration, respectively. The maximum deviation between the predicted result and the calculated result in the case of predicting the weld bead penetration of the TIG welding process is 5.55%. This deviation is acceptable and reliable. In comparison with the experimental results, the ranges of values of the weld bead geometry are within the allowed limitations as shown in Table 13. These results demonstrate the accuracy of mathematical models and artificial intelligence-based models.

In consideration of the research contribution to the classic theory of welding, the mathematical models generated by using the regression technique for analyzing the experiment data enable us to determine the main factors of the welding process parameters which affect the weld bead geometries. From that, we can define the appropriate welding process parameters to ensure weld quality.

From the main factors determined from the generated mathematical models, we developed the artificial intelligence-based models with the input including the main factors of the welding process parameters and the outputs which are the weld bead geometries such as the weld bead width, reinforcement, and penetration. For establishing the artificial intelligence-based models, we used the deep learning neural network technique which uses the experimental data for training networks to obtain the predicted weld bead geometries accurately. The artificial intelligence-based models will be applied for the online monitoring of the welding process to keep the weld quality consistent.

Table 13. Comparison of the values of the weld bead geometry between experiment and prediction.

Welding Process	Weld Bead Geometry	Experimental Results	Predicted Results
TIG welding process	Weld bead width (K_T)	4.4 ÷ 12.9	5.87 ÷ 10.6
	Reinforcement (R_T)	0.3 ÷ 1.4	0.5 ÷ 1.27
	Penetration (P_T)	1.0 ÷ 2.6	1.38 ÷ 1.9
MIG welding process	Weld bead width (K_M)	7.1 ÷ 12.4	7.31 ÷ 12.03
	Reinforcement (R_M)	2.3 ÷ 4.2	2.72 ÷ 3.79
	Penetration (P_M)	1.3 ÷ 2.8	1.53 ÷ 2.43
SMAW welding process	Weld bead width (K_S)	7.4 ÷ 11.3	8.81 ÷ 9.63
	Reinforcement (R_S)	0.6 ÷ 2.0	1.2 ÷ 1.44
	Penetration (P_S)	1.3 ÷ 2.9	1.91 ÷ 2.12

4. Conclusions

In this research, a predictive system was developed for predicting the weld bead geometry in three welding processes. We carried out experiments for SMAW, MIG, and TIG welding processes to obtain the experimental data. From these data, we applied the regression technique and a statistical method for generating the mathematical models showing the relationship between the welding process parameters as the input information and the weld bead geometry as the response. From these mathematical models, the main factors affecting the weld bead shape were determined. These main factors were used as the input parameters for the input layer in the deep learning artificial neural network. The predictive system with four modules was developed using the Python platform. The SMAW, MIG, and TIG modules were implemented using deep learning neural networks for SMAW, MIG, and TIG processes. These results will be applied in developing a virtual welding process system for education carried out by the University of Transport and

Communications, Vietnam. This developed system enables the prediction of the weld joint quality.

Author Contributions: Formal analysis, V.-H.B.; methodology, N.-H.T.; software, V.-T.H.; validation, N.-H.T., V.-H.B. and V.-T.H.; writing—original draft, N.-H.T., V.-H.B. and V.-T.H.; writing—review and editing, N.-H.T., V.-H.B. and V.-T.H. All authors have read and agreed to the published version of the manuscript.

Funding: This research was funded by Vietnam Ministry of Education and Training, grant number: B2021-GHA-01.

Institutional Review Board Statement: Not applicable.

Informed Consent Statement: Not applicable.

Data Availability Statement: Not applicable.

Conflicts of Interest: The authors declare no conflict of interest.

References

1. Mohd, N.C.W.; Ferry, M.; Nik, W.B.W. A study of software approach for predicting weld bead geometry in shielded metal arc welding (SMAW) process. *Appl. Mech. Mater.* **2014**, *554*, 386–390.
2. Ganjigatti, J.P.; Pratihar, D.K.; Choudhury, A.R. Modeling of the MIG welding process using statistical approaches. *Int. J. Adv. Manuf. Technol.* **2008**, *35*, 1166–1190. [CrossRef]
3. Kumar, R.; Saurav, S.K. Modeling of TIG welding process by regression analysis and neural network technique. *Int. J. Mech. Eng. Technol.* **2015**, *6*, 10–27.
4. Shukla, A.A.; Joshi, V.S.; Chel, A.; Shukla, B.A. Analysis of shielded metal arc welding parameter on depth of penetration on AISI 1020 plates using response surface methodology. *Procedia Manuf.* **2018**, *20*, 239–246. [CrossRef]
5. Ghanty, P.; Vasudevan, M.; Mukherjee, D.P.; Pal, N.R.; Chandrasekhar, N.; Maduraimuthu, V.; Bhaduri, A.K.; Barat, P.; Raj, B. Artificial neural network approach for estimating weld bead width and depth of penetration from infrared thermal image of weld pool. *Sci. Tech. Weld. Join.* **2008**, *13*, 395–401. [CrossRef]
6. Nagesh, D.S.; Datta, G.L. Prediction of weld bead geometry and penetration in shielded metal-arc welding using artificial neural networks. *J. Mater. Process. Technol.* **2002**, *123*, 303–312. [CrossRef]
7. Benyounis, K.Y.; Olabi, A.G. Optimization of different welding processes using statistical and numerical approaches—A reference guide. *Adv. Eng. Softw.* **2008**, *39*, 483–496. [CrossRef]
8. Sen, M.; Mukherjee, M.; Pal, T.K. Prediction of weld bead geometry for double pulse gas metal arc welding process by regression analysis. In Proceedings of the 5th International and 26th All India Manufacturing Technology, Design and Research Conference (AIMTDR 2014), Guwahati, India, 12–14 December 2014.
9. Singh, J.; Singh, G. Effects of variation in welding current during SMAW process on A36 mild steel. *Int. J. Res. Appl. Sci. Eng. Technol.* **2022**, *10*, 259–264. [CrossRef]
10. Ranjan, R. Parametric optimization of shielded metal arc welding processes by using factorial design approach. *Int. J. Sci. Res. Publ.* **2014**, *4*. Available online: https://citeseerx.ist.psu.edu/document?repid=rep1&type=pdf&doi=3bff5b16728003f23044819fa6a1ad4f6c275422#page=637 (accessed on 16 February 2022).
11. Ahmed, A.N.; Noor, C.W.M.; Allawi, M.F.; El-Shafie, A. RBF-NN-based model for prediction of weld bead geometry in Shielded Metal Arc Welding (SMAW). *Neural Comput. Appl.* **2018**, *29*, 889–899. [CrossRef]
12. Ali, M.S.; Rao, C.S.; Rao, D.N. Study the effect of shielded metal arc welding process parameters, cryo-treatment and preheating on welding characteristics and modelling by an artificial neural network. *Aust. J. Mech. Eng.* **2014**, *12*, 195–207. [CrossRef]
13. Singh, R.P.; Gupta, R.C.; Sarkar, S.C. Prediction of weld width of shielded metal arc weld under magnetic field using artificial neural networks. *Int. J. Comput. Eng. Res.* **2013**, *3*, 58–64.
14. Pradhan, R.; Joshi, A.P.; Sunny, M.R.; Sarkar, A. Machine learning models for determination of weld bead shape parameters for gas metal arc welded T-joints-A comparative study. *arXiv* **2022**, arXiv:2206.02794.
15. Campbell, S.; Alexander, G.; Norman, M. Artificial neural network prediction of weld geometry performed using GMAW with alternating shielding gases. *Weld. J.* **2012**, *91*, 174–181.
16. Nagesh, D.S.; Datta, G.L. Genetic algorithm for optimization of welding variables for height to width ratio and application of ANN for prediction of bead geometry for TIG welding process. *Appl. Soft Comput.* **2010**, *10*, 897–907. [CrossRef]
17. Ismail, M.I.S.; Okamoto, Y.; Okada, A. Neural network modeling for prediction of weld bead geometry in laser micro-welding. *Adv. Opt. Technol.* **2013**, *2013*, 415837. [CrossRef]
18. Mohd, N.C.W.; Ferry, M.; Gholamhassan, N.; Ahmad, F.; Mohd, A.; Nur, A.R. Prediction of weld bead geometry in SMAW welded plates by using artificial neural network approach. In Proceedings of the 9th International Conference on Marine Technology, Sarawak, Malaysia, 3–4 December 2014.

19. Xiong, J.; Zhang, G.; Hu, J.; Wu, L. Bead geometry prediction for robotic GMAW-based rapid manufacturing through a neural network and a second-order regression analysis. *J. Intell. Manuf.* **2014**, *25*, 157–163. [CrossRef]
20. Kim, I.S.; Lee, S.H.; Yarlagadda, P.K.D.V. Comparison of multiple regression and back propagation neural network approaches in modelling top bead height of multi-pass gas metal arc welds. *Sci. Technol. Weld. Join.* **2003**, *8*, 347–352. [CrossRef]
21. Keshmiri, S.; Zheng, X.; Feng, L.W.; Pang, C.K.; Chew, C.M. Application of deep neural network in estimation of the weld bead parameters. In Proceedings of the IEEE/RSJ International Conference on Intelligent Robots and Systems (IROS), Hamburg, Germany, 28 September–3 October 2015.
22. Majumdar, J.D. Underwater welding—Present status and future scope. *J. Nav. Archit. Mar. Eng.* **2006**, *3*, 39–47. [CrossRef]
23. Kesse, M.A.; Buah, E.; Handroos, H.; Ayetor, G.K. Development of an Artificial Intelligence Powered TIG Welding Algorithm for the Prediction of Bead Geometry for TIG Welding Processes using Hybrid Deep Learning. *Metals* **2020**, *10*, 451. [CrossRef]
24. A First Course in Design and Analysis of Experiments. Available online: http://users.stat.umn.edu/ (accessed on 19 August 2022).
25. Sinha, A.; Kim, D.; Ceglarek, D. Correlation analysis of the variation of weld seam and tensile strength in laser welding of galvanized steel. *Opt. Lasers Eng.* **2013**, *51*, 1143–1152. [CrossRef]
26. Verma, Y. A Complete Understanding of Dense Layers in Neural Networks. Available online: https://analyticsindiamag (accessed on 6 February 2023).
27. ReLU Activation Function. Available online: https://vidyasheela.com (accessed on 6 February 2023).
28. A Gentle Introduction to the Rectified Linear Unit (ReLU). Available online: https://machinelearningmastery.com/rectified-linear-activation-function-for-deep-learning-neural-networks/ (accessed on 6 February 2023).
29. How to Choose Loss Functions When Training Deep Learning Neural Networks. Available online: https://machinelearningmastery.com/how-to-choose-loss-functions-when-training-deep-learning-neural-networks/ (accessed on 6 February 2023).
30. Diederik, P.K.; Jimmy, B. Adam: A method for stochastic optimization. In Proceedings of the 3rd International Conference for Learning Representations, San Diego, CA, USA, 7–9 May 2015.